

Thermal Properties of Deng-Fan-Eckart Potential model using Poisson Summation Approach

C.O.Edet^{1*}, U.S.Okorie^{1&2}, G.Osobonye³, A.N.Ikot¹, G.J.Rampho⁴ and R.Sever⁵.

¹Theoretical Physics Group, Department of Physics, University of Port Harcourt, Port Harcourt-Nigeria.

²Department of Physics, Akwa Ibom State University, Ikot Akpaden, Uyo.-Nigeria

³Department of Physics, Federal College of Education, Omukuru, Rivers State- Nigeria

⁴Department of Physics, University of South Africa.

⁵Department of Physics, Middle East Technical University, 06800, Ankara, Turkey.

ABSTRACT

The Deng-Fan-Eckart (DFE) potential is as good as the Morse potential in studying atomic interaction in diatomic molecules. By using the improved Pekeris-type approximation, to deal with the centrifugal term, we obtain the bound-state solutions of the radial Schrödinger equation with this adopted molecular model via the Factorization Method. With the energy equation obtained, the thermodynamic properties of some selected diatomic molecules(H_2 , CO , ScN and ScF) were obtained using Poisson summation method.. The unnormalized wave function is also derived. The energy spectrum for a set of diatomic molecules for different values of the vibrational n and rotational ℓ are obtained. To show the accuracy of our results, we discuss some special cases by adjusting some potential parameters and also compute the numerical eigenvalue of the Deng-Fan potential for comparison sake. However, it was found out that our results agree excellently with the results obtained via other methods.

Keywords: Deng-Fan molecular potential; Eckart Potential; Pekeris-type approximation; Factorization Method; eigenvalues; eigenfunction; Thermal Properties.

PACS Number(s): 03.65.Ge, 03.65.Fd, 03.65.Pm, 02.30.Gp

*corresponding author email:collinsokonedet@gmail.com

1. INTRODUCTION

An adequate understanding of molecular behavior of two interacting atoms as a function of their relative positions is very pertinent in different fields of Physics and Chemistry. Recently, there has been a great interest in obtaining molecular potential energy functions governing the interaction of two atom (diatomic molecules) [1-5].

In the available literature, numerous efforts have been made by researchers to construct a quasi-precise analytical molecular potential energy function [6-10]. Quite recently, such parameters like the dissociation energy and equilibrium bond length diatomic molecules as explicit parameters has been harnessed by some researchers[11] to construct improved and modified versions for some empirical potential energy functions with more applications, this functions includes; the well-known Rosen-Morse[12], Tietz[13], Frost-Musulin[14], Manning-Rosen[15], Poschl-Teller[16] and Deng-Fan[17] potentials. These authors found that the well-known Tietz potential function is conventionally defined in terms of five parameters but it actually has only four independent parameters. Following the same path, Fu et al. [6] demonstrated that the five-parameter exponential-type potential is identical to the Tietz potential for diatomic molecules. It was observed that the improved five-parameter exponential-type potential can well model the inter-nuclear interaction potential energy curve for the ground electronic state of the carbon monoxide molecule by the utilization of the experimental values of three molecular constants

These modified and or improved molecular potentials have received remarkable attentions. This is due to their various applications in many fields of Physics and Chemistry. Diatomic molecular potentials has been applied to simulate molecular potential energy curves, predict thermo-chemical properties of diatomic molecules[18], calculations of molecular vibrational partition function [19-21] and prediction of enthalpy and entropy of gaseous dimers[22-26].

Berkdemir et al. [27] proposed an improved version of the Kratzer potential[28], Hamzavi et al.[30] proposed an improved expression for the Deng-Fan oscillator potential[17], it was found out that the shifted Deng-Fan was more Morse-like when compared on a plot than the original Deng-Fan oscillator(see. Fig.1 of Ref[30]).The same route was taken by Falaye et al [32] to propose the shifted Tietz-Wei (STW) oscillator. They shifted the well-known Tietz-Wei potential [33-36] by D_e . In their presentation, it was noted that STW is as good as the traditional Morse potential [3, 37] in simulating the atomic interaction in diatomic molecules.

Several methods have been adopted to study these potentials in the relativistic and non-relativistic regime, these includes the Nikiforov Uvarov method[38,39], Factorization Method[40], Modified Factorization Method[20, 21],Asymptotic Iteration Method(AIM)[41, 42] and Supersymmetric Quantum Mechanics(SUSYQM)[43, 44], Exact Quantization Rule[45-49], Proper quantization Rule[50-54] and Formula Method[55] amongst others.

These great attempts were made in a quest to find the most suitable molecular potential for the description of diatomic molecules. Motivated by works in Refs. [27, 30 and 32], we adopt the Deng-Fan-Eckart Potential(DFEP) proposed by Ikot et al. [59] to study interatomic interactions of diatomic molecules .This potential is given by[56]

$$V(r) = D_e \left(1 - \frac{b}{(e^{\alpha r} - 1)} \right)^2 - \frac{V_1 e^{-\alpha r}}{(1 - e^{-\alpha r})} + \frac{V_2 e^{-\alpha r}}{(1 - e^{-\alpha r})^2} \quad (1)$$

$b = e^{\alpha r_e} - 1$

where r_e is the molecular bond length, D_e is the dissociation energy, r is the inter-nuclear distance, α the range of the potential well, V_1 and V_2 are the potential strengths. This potential is just a superposition of the Deng-Fan and Eckart potentials. The shape of this potential is shown in Fig. 1.

Ikot et al [56] solved the Dirac equation under spin and pseudo-spin symmetries Deng–Fan-Eckart potential with Coulomb-like and Yukawa-like tensor interaction terms. The energy equation was obtained by using the Nikiforov–Uvarov method. This study is an extension of the work of ref. [56].

The thermal properties for the Deng–Fan-Eckart potential are also studied in this work. These include vibrational partition function, vibrational mean energy, vibrational mean free energy, vibrational entropy, etc. Prior to now, different authors have investigated the thermodynamic properties for some quantum mechanical systems [19-22].

The objective of this study is in three fold; firstly, we solve the Schrodinger with the DFE potential using the Factorization method, we apply the energy equation obtained to study atomic behavior in some selected diatomic molecules and also study the thermodynamic properties of this potential for some selected molecules.

The scheme of our research article is as follows. In the next section, we solve the radial Schrödinger equation with the Deng-Fan-Eckart Potential using the Factorization method [40] and in section 3, we obtain the thermodynamic properties for the diatomic molecules which will be calculated using the expression for the partition function. In section 4, we obtain the rotational-vibrational energy spectrum for some diatomic molecules with numerical results and discussion. In section 5, we present special case of the potential under consideration. Finally, in section 6 we give concluding remark.

2. Energy levels and Wavefunction

The radial part of the Schrödinger equation is given by[57];

$$\frac{d^2\psi(r)}{dr^2} + \frac{2\mu}{\hbar^2} \left[E_{nl} - V(r) - \frac{\hbar^2 \ell(\ell+1)}{2\mu r^2} \right] \psi(r) = 0 \quad (2)$$

Considering Deng-Fan-Eckart potential (Eq.(1)), we obtain the radial Schrödinger equation, Eq.(2) is rewritten as follows:

$$\frac{d^2\psi(r)}{dr^2} + \frac{2\mu}{\hbar^2} \left[E_{n\ell} - \left(D_e + \frac{D_e b^2 e^{-2\alpha r}}{(1-e^{-\alpha r})^2} - \frac{2D_e b e^{-\alpha r}}{(1-e^{-\alpha r})} - \frac{V_1 e^{-\alpha r}}{(1-e^{-\alpha r})} + \frac{V_2 e^{-\alpha r}}{(1-e^{-\alpha r})^2} \right) - \frac{\hbar^2 \ell(\ell+1)}{2\mu r^2} \right] \psi(r) = 0 \quad (3)$$

This equation cannot be solved analytically for $\ell \neq 0$ due to the centrifugal term. Therefore, we must use an approximation to the centrifugal term. We use the following approximation [30]

$$\frac{1}{r^2} \approx \alpha^2 \left[d_0 + \frac{e^{\alpha r}}{(1-e^{\alpha r})^2} \right] \quad (4)$$

It has been shown extensively in literature that this approximation scheme approximates the centrifugal barrier better than the well-known Greene and Aldrich[58] approximation scheme[31]. In the limiting case when $\alpha r \rightarrow 1$, the value of the dimensionless constant $d_0 = \frac{1}{12}$

and the screening parameter α approaches zero, Eq.(4) reduces to $\frac{1}{r^2}$.

Inserting Eqs. (4) into Eq. (3) where we have the $\frac{1}{r^2}$ term, we have;

$$\frac{d^2\psi(r)}{dr^2} + \frac{2\mu}{\hbar^2} \left[E_{n\ell} - \left(D_e + \frac{D_e b^2 e^{-2\alpha r}}{(1-e^{-\alpha r})^2} - \frac{2D_e b e^{-\alpha r}}{(1-e^{-\alpha r})} - \frac{V_1 e^{-\alpha r}}{(1-e^{-\alpha r})} + \frac{V_2 e^{-\alpha r}}{(1-e^{-\alpha r})^2} \right) - \frac{\hbar^2 \ell(\ell+1)\alpha^2}{2\mu} \left(d_0 + \frac{e^{\alpha r}}{(1-e^{\alpha r})^2} \right) \right] \psi(r) = 0 \quad (5)$$

For Mathematical simplicity, let's introduce the following dimensionless notations;

$$\begin{aligned} -\varepsilon^2 &= \frac{2\mu(E_{n\ell} - D_e)}{\hbar^2 \alpha^2}, \eta_1 = \frac{2\mu D_e b^2}{\hbar^2 \alpha^2}, \\ \eta_2 &= \frac{4\mu D_e b}{\hbar^2 \alpha^2}, \beta_1 = \frac{2\mu V_1}{\hbar^2 \alpha^2}, \beta_2 = \frac{2\mu V_2}{\hbar^2 \alpha^2} \\ \gamma &= \ell(\ell+1). \end{aligned} \quad (6)$$

Hence, Eq.(5) can be rewritten in a less ambiguous form as;

$$\frac{d^2\psi(r)}{dr^2} + \left[-\varepsilon^2 (1-e^{-\alpha r})^2 - \eta_1 e^{-2\alpha r} + \eta_2 e^{-\alpha r} (1-e^{-\alpha r}) + \beta_1 e^{-\alpha r} (1-e^{-\alpha r}) - \beta_2 e^{-\alpha r} - \gamma e^{-\alpha r} - \gamma d_0 (1-e^{-\alpha r})^2 \right] \psi(r) = 0 \quad (7)$$

Using the coordinate transformation $s = e^{-\alpha r}$, Eq.(7) translates to;

$$\frac{d^2\psi(s)}{ds^2} + \frac{1}{s} \frac{d\psi(s)}{ds} + \frac{1}{s^2 (1-s)^2} \left[-(\varepsilon^2 + \eta_1 + \eta_2 + \beta_1 + \gamma d_0) s^2 + (2\varepsilon^2 + \eta_2 + \beta_1 - \beta_2 - \gamma + 2\gamma d_0) s - (\varepsilon^2 + \gamma d_0) \right] \psi(s) = 0 \quad (8)$$

If we consider the boundary conditions

$$s \Rightarrow \begin{cases} 0, & \text{when } r \rightarrow \infty, \\ 1, & \text{when } r \rightarrow 0, \end{cases} \quad (9)$$

with $\psi(s) \rightarrow 0$, we take the following radial wave functions of the form

$$\psi(s) = s^\lambda (1-s)^\omega f(s) \quad (10)$$

where

$$\lambda = \sqrt{\varepsilon^2 + \gamma d_0} \quad (11)$$

$$\omega = \frac{1}{2} + \sqrt{\frac{1}{4} + \eta_1 + \beta_2 + \gamma} \quad (12)$$

On substitution of Eq. (10) into Eq. (8) leads to the following hypergeometric equation:

$$s(1-s) \frac{d^2 f(s)}{ds^2} + [(2\lambda+1) - (2\lambda+2\omega+1)s] \frac{df(s)}{ds} - \left[\frac{(\lambda+\omega)^2}{-\varepsilon^2 + \eta_1 + \eta_2 + \beta_1 + \gamma d_0} \right] f(s) = 0 \quad (13)$$

whose solutions are nothing but the hypergeometric functions

$$f(s) = {}_2F_1(a, b; c; s) \quad (14)$$

where

$$\begin{aligned} a &= (\lambda + \omega) - \sqrt{\varepsilon^2 + \eta_1 + \eta_2 + \beta_1 + \gamma d_0} \\ b &= (\lambda + \omega) + \sqrt{\varepsilon^2 + \eta_1 + \eta_2 + \beta_1 + \gamma d_0} \\ c &= 2\lambda + 1 \end{aligned} \quad (15)$$

By considering the finiteness of the solutions, the quantum condition is given by

$$(\lambda + \omega) - \sqrt{\varepsilon^2 + \eta_1 + \eta_2 + \beta_1 + \gamma d_0} = -n, \quad n = 0, 1, 2, \dots \quad (16)$$

from which we obtain

$$\varepsilon^2 = -\gamma d_0 + \frac{1}{4} \left(\frac{\left(n + \frac{1}{2} + \sqrt{\frac{1}{4} + \eta_1 + \beta_2 + \gamma} \right)^2 - \eta_1 - \eta_2 - \beta_1}{\left(n + \frac{1}{2} + \sqrt{\frac{1}{4} + \eta_1 + \beta_2 + \gamma} \right)} \right)^2 \quad (17)$$

Thus, if one substitutes the value of the dimensionless parameters in Eq.(6) into Eq.(17), we obtain the solutions as follows:

$$E_{n\ell} = D_e + \frac{\hbar^2 \alpha^2 \ell(\ell+1) d_0}{2\mu} - \frac{\hbar^2 \alpha^2}{2\mu} \left(\frac{(n+\nu)^2 - \frac{2\mu D_e b^2}{\hbar^2 \alpha^2} - \frac{4\mu D_e b}{\hbar^2 \alpha^2} - \frac{2\mu V_1}{\hbar^2 \alpha^2}}{2(n+\nu)} \right)^2 \quad (18)$$

Where,

$$\nu = \frac{1}{2} + \frac{1}{2} \sqrt{(2\ell+1)^2 + \frac{8\mu D_e b^2}{\hbar^2 \alpha^2} + \frac{8\mu V_1}{\hbar^2 \alpha^2}} \quad (19)$$

The corresponding unnormalized wave function is obtain as

$$\psi(s) = N_{nl} s^{\sqrt{\varepsilon^2 + \gamma d_0}} (1-s)^{\frac{1}{2} + \sqrt{\frac{1}{4} + \eta_l + \beta_2 + \gamma}} {}_2F_1(-n, n+2(\lambda+\omega); 2\lambda+1; s) \quad (20)$$

3. THERMAL PROPERTIES OF DFEP

The vibrational partition function can be calculated with the aid of direct summation over all possible vibrational energy levels at a given temperature T to be[19]

$$Z(\beta) = \sum_{n=0}^{n_{\max}} e^{-\beta E_{nl}}, \quad \beta = \frac{1}{k_B T} \quad (21)$$

Here, k_B is the Boltzmann constant and E_{nl} is the rotational-Vibrational energy of the nth bound state.

We can rewrite eq. (18) to be of the form

$$E_{nl} = P_1 - \frac{\hbar^2 \alpha^2}{2\mu} \left[\frac{(n+v)}{2} + \frac{P_2}{2(n+v)} \right]^2 \quad (22)$$

where

$$P_1 = D_e + \frac{\hbar^2 \alpha^2 l(l+1) d_0}{2\mu}; \quad P_2 = - \left(\frac{2\mu D_e b^2}{\hbar^2 \alpha^2} + \frac{4\mu D_e b}{\hbar^2 \alpha^2} + \frac{2\mu V_1}{\hbar^2 \alpha^2} \right) \quad (23)$$

We substitute eq. (22) into eq. (21) to have

$$Z(\beta) = \sum_{n=0}^{n_{\max}} e^{-\beta \left[P_1 - \frac{\hbar^2 \alpha^2}{2\mu} \left(\frac{(n+v)}{2} + \frac{P_2}{2(n+v)} \right)^2 \right]} \quad (24)$$

where

$$n_{\max} = \sqrt{P_2} - v \quad (25)$$

We adopt the Poisson summation formula given as [59]

$$\sum_{n=0}^{n_{\max}} f(x) = \frac{1}{2} [f(0) - f(n_{\max} + 1)] + \sum_{m=-\infty}^{\infty} \int_0^{n_{\max} + 1} f(y) e^{-i2\pi m y} dy \quad (26)$$

But, for the lower order approximation, the Poisson summation formula reduces to [59]

$$\sum_{n=0}^{n_{\max}} f(x) = \frac{1}{2} [f(0) - f(n_{\max} + 1)] + \int_0^{n_{\max} + 1} f(y) dy \quad (27)$$

By the application of eq. (27) for the partition function of eq. (24), we obtain

$$Z(\beta) = \frac{1}{2} \left[e^{-\beta(P_1 - q_1 q_2^2)} - e^{-\beta(P_1 - q_1 q_3^2)} + \int_0^{n_{\max}} \left(e^{-L_1 \beta - \frac{L_2 \beta}{\rho^2} - L_3 \beta \rho^2} \right) d\rho \right] \quad (28)$$

where

$$\begin{aligned} q_1 &= \frac{\hbar^2 \alpha^2}{2\mu}; \quad q_2 = \left(\frac{P_2}{2n_{\max}} + \frac{n_{\max}}{2} \right); \quad q_3 = \left(\frac{P_2}{2(n_{\max} + 1 + v)} + \frac{(n_{\max} + 1 + v)}{2} \right); \\ \rho &= y + v; \quad L_1 = \frac{\hbar^2 \alpha^2 P_2^2}{4\mu} - P_1; \quad L_2 = \frac{\hbar^2 \alpha^2 P_2^2}{8\mu}; \quad L_3 = \frac{\hbar^2 \alpha^2}{4\mu} \end{aligned} \quad (29)$$

We therefore use the Maple software to evaluate the integral in eq. (36), thus obtaining the Poisson summation rotational-vibrational partition function for the diatomic molecules with DFEP models as

$$Z(\beta) = \frac{1}{2} \left[e^{-\beta(P_1 - q_1 q_2^2)} - e^{-\beta(P_1 - q_1 q_3^2)} + e^{-L_3 \beta \rho^2 - L_1 \beta} \sqrt{L_2 \beta} \left(\frac{2n_{\max} e^{-\frac{L_2 \beta}{n_{\max}^2}}}{\sqrt{L_2 \beta}} + \frac{2\sqrt{L_2 \beta} \sqrt{\pi} \operatorname{erf}\left(\frac{\sqrt{L_2 \beta}}{n_{\max}}\right)}{\sqrt{L_2 \beta}} - 2\sqrt{\pi} \right) \right] \quad (30)$$

The imaginary error function can be defined as [21]

$$\operatorname{erfi}(z) = i \operatorname{erf}(z) = \frac{2}{\sqrt{\pi}} \int_0^z e^{u^2} du \quad (31)$$

Thermodynamic functions such as Helmholtz free energy, $F(\beta)$, entropy, $S(\beta)$, internal energy, $U(\beta)$, and specific heat, $C_v(\beta)$, functions can be obtained from the partition function (30) as follows [20];

$$F(\beta) = -\frac{1}{\beta} \ln Z(\beta) \quad (32)$$

$$S(\beta) = -k_\beta \frac{\partial F(\beta)}{\partial \beta} \quad (33)$$

$$U(\beta) = -\frac{\partial (\ln Z(\beta))}{\partial \beta} \quad (34)$$

$$C_v = k_\beta \frac{\partial U(\beta)}{\partial \beta} \quad (35)$$

4. Applications

To show the accuracy of energy equation obtained in this work, we calculate the energy levels using Eq.(18) for different quantum numbers n and ℓ with for four diatomic molecules(H_2 , CO , ScN and ScF). In our numerical computations, we have used spectroscopic parameters shown in Table 1 and the following conversions: $1 \text{ amu} = 931.494028 \frac{\text{MeV}}{c^2}$, $1 \text{ cm}^{-1} = 1.239841875 \times 10^{-4} \text{ eV}$ and $\hbar c = 1973.29 \text{ eV \AA}$.

The numerical values of these energies for different vibrational and rotational quantum numbers are presented in Table 4. To further validate our results, we have also computed the energy eigenvalues of the Deng-Fan potential using the reduced energy equation given in Eq. (22) as a special case. Our results shown in Tables 2 and 3 are in good agreement with the results given in Ref. [31].

Figs. 1 shows a comparison between DFE diatomic molecular potential, and the Morse potential using the parameters set for H_2 diatomic molecule. As it can be seen from this plot, the Deng-Fan-Eckart and the Morse potentials are very close to each other for large values of r in the regions $r \approx r_e$ and $r > r_e$, but they are very different at $r = 0$. This implies that the Deng-Fan-Eckart potential is as good as the Morse potential in simulating the molecular interaction for diatomic molecules. The shape of this potential is shown in Fig. 1 for different molecules. Fig. 3 shows the energy eigenvalues variation with dissociation energy for various vibrational quantum states. It can be easily observed from Fig. (3) that the dissociation energy increases directly as the energy increases. Fig. 4 shows the energy eigenvalues variation with equilibrium bond length for various vibrational quantum numbers. In Fig. 4, the minimum value of the energy is observed when the value of r_e is in the region of $0.1 - 0.2 \text{\AA}$. Beyond this region, the energy begins to decrease abruptly. More so, an asymptotic behavior is observed in the curve representing the 2p state. Fig. 5 shows the energy eigenvalues variation with screening parameter for various vibrational quantum numbers. From the plot, it can be seen that there is a uniform convergence of the energy curves at the point where $\alpha \approx 0.1$ (i.e. in the low screening region) and $E_{nl} \approx 50 \text{ eV}$. Beyond this region, the curves uniformly diverge and there is a sharp decrease in energy as α increases except in the 2p state, where the energy was almost constant. Figure 6 shows Energy eigenvalues variation with parameter V_1 for various vibrational quantum numbers. All curves representing the energy states show a uniform decrease in energy as V_1 increases. In Fig. 7 shows the energy eigenvalues variation with parameter V_2 for various vibrational quantum numbers and the energy increases monotonically with V_2 .

Figure 8 shows the energy eigenvalues variation with dissociation energy for various diatomic molecules. It is seen that the dissociation energy increases directly as the energy increases for all diatomic molecules except for ScN molecule which shows an almost-linear trend. Figure 9 shows the variation of the energy of the system with the equilibrium bond length for the four diatomic molecules under study. It's seen that in the low region of r_e , the energy drops to almost zero. Beyond $r_e \approx 0$, we notice a sharp rise and this continues in a quasi-linear manner. Figure 10 shows the energy variation with the screening parameter α . In the low screening region ($\alpha \approx 0-1$), we observe a sharp rise in the energy, beyond this point, there is a sharp decrease in the energy eigenvalue and this continues as the screening parameter increase. For ScF molecule

curve, we observe a quasi-asymptotic behavior. Figures 11 and 12 shows the variation of the energy of the system with parameters V_1 and V_2 for different molecules studied. It is seen that a linear relationship exist between the energy and the parameters. Figure 13 explicitly shows the energy eigenvalues variation with the particle mass μ for various diatomic molecules. It can be seen that in the region $\mu \approx 0 - 0.1 \text{ a.m.u}$, the energy eigenvalue drops sporadically. This continues in a linear trend. The energy is only high in the region where the mass is very low but decreases as the particle's mass increases. The energy is very similar for $0.2 < \mu < 1.0$.

In Fig. 14 we show the vibrational partition function variation with temperature for various diatomic molecules. It can be seen that the partition function is almost invariant with increasing Temperature for the H_2 molecule. For the other three molecules, we observed that in the region $\beta \approx 0 - 1 \times 10^{-12}$, the partition function is very low, beyond this point, it rises abruptly. Fig. 15 shows the Vibrational free energy variation with temperature for various diatomic molecules. It is seen that the vibrational free energy increases monotonically with increasing Temperature. Fig. 16 and 17 shows the Vibrational mean energy and entropy variation with temperature for various diatomic molecules. Again, it can be seen that the Vibrational mean energy and entropy is almost invariant with increasing Temperature for the H_2 molecule. For other three molecules considered, the Vibrational mean energy and entropy decreases as the Temperature increases. Fig. 18 shows the vibrational specific heat capacity variation with temperature for various diatomic molecules. In like manner, the vibrational specific heat capacity is invariant with increasing Temperature for the H_2 molecule. For other three molecules, we observe that the vibrational specific heat capacity increases sporadically as the temperature increases.

5. Special cases

In this section, we make some adjustments of constants in Eq. (1) and Eq. (18) to have the following cases:

Deng-Fan Potential

If we set V_1 and V_2 equal to zero, the DFE potential model (Eq. 1) reduces to the Deng-Fan potential

$$V(r) = D_e \left(1 - \frac{b}{(e^{\alpha r} - 1)} \right)^2 \quad (36)$$

$$b = e^{\alpha r_e} - 1$$

In like manner, Eq.(18) reduces to the energy equation for the Deng-Fan potential

$$E_{n\ell} = D_e + \frac{\hbar^2 \alpha^2 \ell(\ell+1) d_0}{2\mu} - \frac{\hbar^2 \alpha^2}{2\mu} \left\{ \frac{\left(n + \frac{1}{2} + \frac{1}{2} \sqrt{(2\ell+1)^2 + \frac{8\mu D_e b^2}{\hbar^2 \alpha^2}} \right)^2 - \frac{2\mu D_e b^2}{\hbar^2 \alpha^2} - \frac{4\mu D_e b}{\hbar^2 \alpha^2}}{\left(2n + 1 + \sqrt{(2\ell+1)^2 + \frac{8\mu D_e b^2}{\hbar^2 \alpha^2}} \right)} \right\} \quad (37)$$

Eq.(37) is in agreement with Eq. (29) of ref.[31] who solved the Schrodinger equation with this potential using the NU method with the same approximation. If $d_0 = 0$, the energy reduces to the result obtained in Eq.(20) of ref.[60].

Eckart Potential

If we set D_e equal to zero, the DFE potential model (Eq. 1) reduces to the Deng-Fan potential

$$V(r) = -\frac{V_1 e^{-\alpha r}}{(1-e^{-\alpha r})} + \frac{V_2 e^{-\alpha r}}{(1-e^{-\alpha r})^2} \quad (38)$$

$$E_{nl} = \frac{\hbar^2 \alpha^2 \ell(\ell+1) d_0}{2\mu} - \frac{\hbar^2 \alpha^2}{2\mu} \left(\frac{\left(n + \frac{1}{2} + \frac{1}{2} \sqrt{(2\ell+1)^2 + \frac{8\mu V_2}{\hbar^2 \alpha^2}} \right)^2 - \frac{2\mu V_1}{\hbar^2 \alpha^2}}{\left(2n+1 + \sqrt{(2\ell+1)^2 + \frac{8\mu V_2}{\hbar^2 \alpha^2}} \right)} \right)^2 \quad (39)$$

If $d_0 = 0$, Eq.(39) reduces to the energy equation obtained in Eq.(31) of ref.[61].

Hulthen Potential

If we set D_e and V_2 equal to zero, the DFE potential model (Eq. 1) reduces to the Deng-Fan potential

$$V(r) = -\frac{V_1 e^{-\alpha r}}{(1-e^{-\alpha r})} \quad (40)$$

$$E_{nl} = \frac{\hbar^2 \alpha^2 \ell(\ell+1) d_0}{2\mu} - \frac{\hbar^2 \alpha^2}{2\mu} \left(\frac{(n+\ell+1)^2 - \frac{2\mu V_1}{\hbar^2 \alpha^2}}{2(n+\ell+1)} \right)^2 \quad (41)$$

Eq.(41) is identical with the energy eigenvalues formula given in Eq. (36) of ref.[62], Eq. (32) of ref.[63], Eq. (24) of ref.[64] and Eq. (28) of [65].

6. Conclusion

In this article, we have solved the Schrodinger equation using factorization method and suitable approximation to overcome the centrifugal barrier. We have expressed the solutions by the generalized hypergeometric functions ${}_2F_1(a, b; c; s)$. We have also presented the ro-vibrational energy spectra with the Deng-Fan-Eckart potential model for some diatomic molecules. Computation of energies have been done numerically and the results discussed extensively using plots. In detail, we evaluated the vibrational partition functions $Z(\beta)$ which we used to study the thermodynamics properties of vibrational mean energy $U(\beta)$, vibrational entropy $S(\beta)$, vibrational mean free energy $F(\beta)$ and vibrational specific heat capacity $C(\beta)$ for some selected diatomic molecules. We discussed some special cases by adjusting the potential

parameters and compute the numerical energy spectra for the Deng-Fan potential. It was found that our results agree with the existing literature. More so, we also found out that the Deng-Fan-Eckart potential can effectively describe the vibrational energy levels of diatomic molecules. Recently, there has been investigations by some researchers reporting some interesting description of internal vibrations of diatomic molecules. Worthy to point out are the works that have successfully predicted the thermodynamic properties for some diatomic gases and gaseous dimmers, including CO, N₂, Cl₂ and gaseous sodium dimer and lithium dimer [68-74]. Finally, this study has many applications in different areas of physics and chemistry such as atomic physics, molecular physics and chemistry amongst others

REFERENCES

- [1] B.J. Falaye, K.J. Oyewumi, S. M. Ikhdaire, M. Hamzavi, Phys. Scr. **89**(2014)115204.
- [2]B. J. Falaye, K. J. Oyewumi, F. Sadikoglu, M. Hamzavi, S. M. Ikhdaire, J. Theor. Comput. Chem.**14** (2015)1550036.
- [3] H. B. Liu, L. Z. Yi, C. S. Jia, J. Math. Chem. **56** (2018) 2982.
- [4] R. Khordad, A. Ghanbari, Comp. & Theo Chem **1155** (2019) 1
- [5] B.J. Falaye, S.M. Ikhdaire, M. Hamzavi, J. Math. Chem. **53** (2015) 1325.
- [6] K. X. Fu,Meng Wang, C. S. Jia, Commun. Theor. Phys. **71** (2019) 103
- [7] G. D. Zhang, J. Y. Liu, L. H. Zhang, W. Zhou, C. S. Jia, Phys. Rev. A **86** (2012) 062510.
- [8] P. Q. Wang, L. H. Zhang, C. S. Jia, J. Y. Liu, Mol. J. Spectrosc. **274** (2012) 5.
- [9] G. C. Liang, H. M. Tang, C. S. Jia, Comput. Theor. Chem. **1020** (2013) 170.
- [10] C. S. Jia, L. H. Zhang, X. L. Peng, Int. J. Quantum. Chem. **117** (2017) e25383.
- [11]C.S. Jia, Y.F. Diao, X.J. Liu, P.Q. Wang, J.Y. Liu, G.D. Zhang, J. Chem. Phys. **137**(2012)014101.
- [12] N. Rosen, P. M. Morse, Phys. Rev. **42** (1932) 210.
- [13] T. Tietz, J. Chem. Phys. **38** (1963) 3036.
- [14] A. A. Frost, B. Musulin, J. Chem. Phys. **22**(1954)1017.
- [15] M. F. Manning, N. Rosen, Phys. Rev. 44 (1933) 951.
- [16] G. Poschl, E. Teller, Z. Physik **83** (1933) 143.
- [17] Z. H. Deng, Y. P. Fan, Shandong Univ. J. **7** (1957) 162.
- [18]C. O. Edet, U. S. Okorie, A. T. Ngiangia, A. N. Ikot,Ind. J. Phys. (2019)
- [19] U. S. Okorie, E. E. Ibekwe, A. N. Ikot, M. C. Onyeaju, E. O. Chukwuocha, J. Kor. Phys. Soc. **73**(2018)1211.

- [20] U. S. Okorie, A. N. Ikot, M. C. Onyeaju, E. O. Chukwuocha, Rev. Mex. de Fis. **64** (2018) 608.
- [21] Z. Ocak, H. Yanar, M. Saltı, O. Aydoğdu, Chem. Phys. **513** (2018) 252
- [22] C. S. Jia, C. W. Wang, L. H. Zhang, X. L. Peng, H. M. Tang, J. Y. Liu, Y. Xiong, R. Zeng, Chem. Phys. Lett. **692**(2018)57.
- [23] X. L. Peng, R. Jiang, C. S. Jia, L. H. Zhang, Y. L. Zhao, Chem. Eng. Sci. **190**(2018)122.
- [24] R. Jiang, C. S. Jia, Y. Q. Wang, X. L. Peng, L. H. Zhang, Chem. Phys. Lett. **715**(2019)186.
- [25] C. S. Jia, C. W. Wang, L. H. Zhang, X. L. Peng, H. M. Tang, R. Zeng, Chem. Eng. Sci. **183**(2018)26.
- [26] C. S. Jia, R. Zeng, X. L. Peng, L. H. Zhang, Y. L. Zhao, Chem. Eng. Sci. **190**(2018)1.
- [27] C. Berkdemir, J. Han, Chem. Phys. Lett. **409**(2005)203.
- [28] A. Kratzer, Z. Phys. **3**(1920)289.
- [29] C. O. Edet , K. O. Okorie, H. Louis, N. A. Nzeata-Ibe, Ind. J. Phys. (2018)
- [30] M. Hamzavi, S. M. Ikhdaire, K. E. Thylwe, J. Math. Chem. **51** (2013) 227.
- [31] K. J. Oyewumi, O. J. Oluwadare, K. D. Sen, O. A. Babalola, J. Math. Chem. **51** (2013) 976.
- [32]B. J. Falaye, S. M. Ikhdaire, M. Hamzavi, J. Theor. Appl. Phys. **9** (2015) 151.
- [33] M. Hamzavi, A. A. Rajabi, K. E. Thylwe, Int. J. Quant. Chem. **112** (2011) 1
- [34] W. Hua, Phys. Rev. A. **42**(1990)2524.
- [35] F.J.Gordillo-Va'zquez, J.A. Kunc, J. Appl. Phys. **84**(1998)4693.
- [36] G.H.Sun,S.H.Dong, Commun. Theor. Phys. **58**(2012)195.
- [37] P. M. Morse, Phys. Rev. **34** (1929) 57.
- [38] A. F. Nikiforov, V. B. Uvarov, Special Functions of Mathematical Physics (ed.) A. Jaffe (Germany: Birkhauser Verlag Basel) p 317 (1998).
- [39] C. Berkdemir, Application of the Nikiforov–Uvarov Method in Quantum Mechanics. In Pahlavani MR (ed), Theoretical Concept of Quantum Mechanics, 11 (2012).
- [40]S. H. Dong, Factorization Method in Quantum Mechanics, Springer, 2007.
- [41]I. A. Assi, A. J. Sous,A. N.Ikot, Euro. Phys. J. plus **132** (2017)525
- [42]A. N. Ikot, E. O. Chukwuocha,M. C.Onyeaju, C. A. Onate,B. I. Ita,M. E.Udoh, Pramana J. Phys, **90** (2018) 22.

- [43] C. A. Onate,M. C.Onyeaju, A. N. Ikot,O.Ebomwonyi, Euro.Phys. J. plus **132** (11) (2017) 462.
- [44] A. N.Ikot, H. Hassanabadi,E. Maghsoodi,S.Zarrinkamar,Phys. Part. Nucl. Lett.**11** (2015) 432.
- [45] W.C. Qiang, S.H. Dong, Euro. Phys. Lett. **89** (2010)10003.
- [46] S. H. Dong, A. Gonzalez-Cisneros, Ann. Phys. **323**(2008)1136.
- [47] X. Y. Gu, S. H. Dong, Z. Q. Ma, J. Phys. A: Math. Theor. **42**(2009)035303.
- [48] S. M. Ikhdaire, J. Abu-Hasna, Phys. Scr. **83**(2011)025002.
- [49] S.H. Dong, D. Morales, J. Garcia-Ravelo. Int. J. Mod. Phys. E **16**(2007)189.
- [50] F.A. Serrano, X.Y. Gu, S.H. Dong, J. Math. Phys. **51**(2010)082103.
- [51] B.J. Falaye, S.M. Ikhdaire, M. Hamzavi, J. Math. Chem. **53** (2015) 1325.
- [52] S. H. Dong, M. Cruz-Irisson, J. Math. Chem. **50**(2012)881.
- [53]O.J. Oluwadare, K.J. Oyewumi, Eur. Phys. J. Plus **133** (2018) 422.
- [54] X.Y. Gu, S.H. Dong, J. Math. Chem. **49**(2011)2053.
- [55] B.J. Falaye, S.M. Ikhdaire, M. Hamzavi, Few Body Sys. **56**(2015) 63.
- [56] A. N. Ikot, S. Zarrinkamar, B. H. Yazarloo, H. Hassanabadi, Chin. Phys. **23**(10) (2014) 100306.
- [57] M. E. Udoh, U. S. Okorie, M. I. Ngwueke, E. E. Ituen and A. N. Ikot, J. Mol. Mod.**25**(2019)1.
- [58] R. L. Greene, C. Aldrich, Phys. Rev. A **14**(1976)2363.
- [59] X. Q. Song, C. W. Wang and C. S. Jia Chem. Phys. Lett **673** (2017) 50
- [60]S. H. Dong, X. Y. Gu, Journal of Physics: Conference Series **96** (2008) 012109.
- [61] J. Gao, M. C. Zhang, Chin. Phys. Lett. **33**(1) (2016) 010303.
- [62]S.M. Ikhdaire, Eur. Phys. J. A **39**(2009) 307.
- [63] O. Bayrak, G. Kocak, I. Boztosun,J. Phys. A: Math. Gen. **39** (2006) 11521.
- [64] C. S. Jia, J. Y. Liu, P. Q. Wang, Phys. Lett. A **372** (2008) 4779.
- [65]S.M. Ikhdaire, R. Sever, J. Math. Chem. **42**(2007)461.
- [66] K.J. Oyewumi, B.J. Falaye, C.A. Onate, O. J. Oluwadare, W.A. Yahya Mol. Phys. **112**(1) (2014) 127.

- [67] W. Lucha, F. F. Schoberl, Int. J. Mod. Phys. C **10**(1999)607.
- [68] M. Buchowiecki, , Chem. Phys. Lett. **692** (2018) 236
- [69] J. F. Du, P. Guo and C. S. Jia. J Math Chem **52** (2014) 2559
- [70] C. S. Jia , L. H. Zhang and C.W. Wang. Chem. Phys. Lett. **667** (2017) 211
- [71] C-S. Jia, C-W. Wang, L-H. Zhang, X-L. Peng, R. Zeng, X-T. You, Chem. Phys. Lett. **676** (2017) 150
- [72] C-S. Jia, X-T. You, J-Y. Liu, L-H. Zhang, X-L. Peng, Y-T. Wang, L-S. Wei, Chem. Phys. Lett. **717** (2019) 16
- [73] C-S. Jia, L-H. Zhang, X-L. Peng, J-X. Luo, Y-L. Zhao, J-Y. Liu, J-J. Guo, L-D. Tang, Chem. Eng. Sci. **202** (2019) 70
- [74] R. Jiang, C-S. Jia, Y-Q. Wang, X-L. Peng, L-H. Zhang, Chem. Phys. Lett. **726** (2019) 83
- [75]. C.O. Edet, K.O. Okorie, H. Louis, N.A. Nzeata-Ibe, Any l-state solutions of the Schrodinger equation interacting with Hellmann-Kratzer potential model. Indian J. Phys. 94, 243–251 (2020). <https://doi.org/10.1007/s12648-019-01467-x>

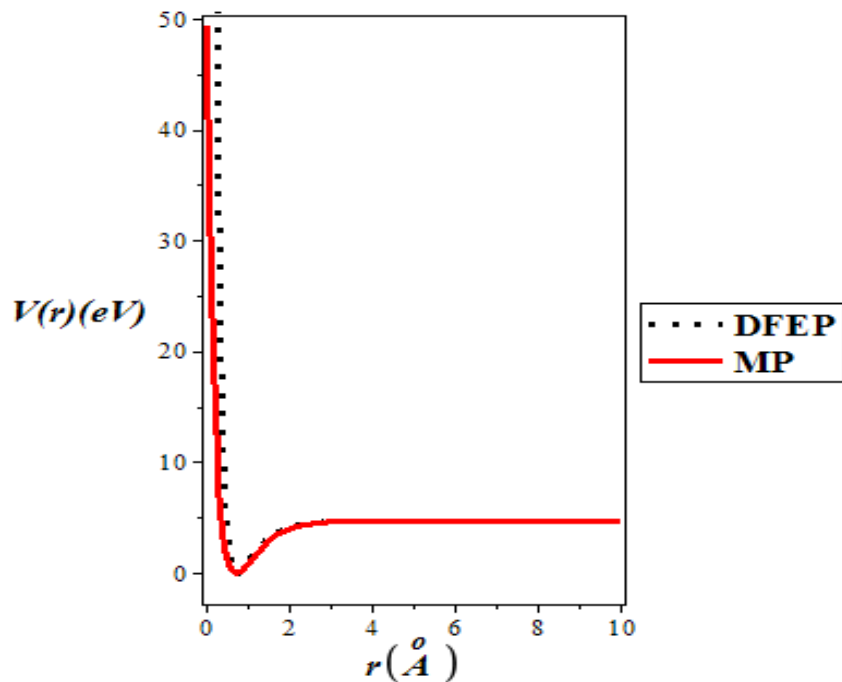


Figure 1: Shape of the Deng-Fan-Eckart potential model and Morse oscillator potentials for H_2 diatomic molecule.

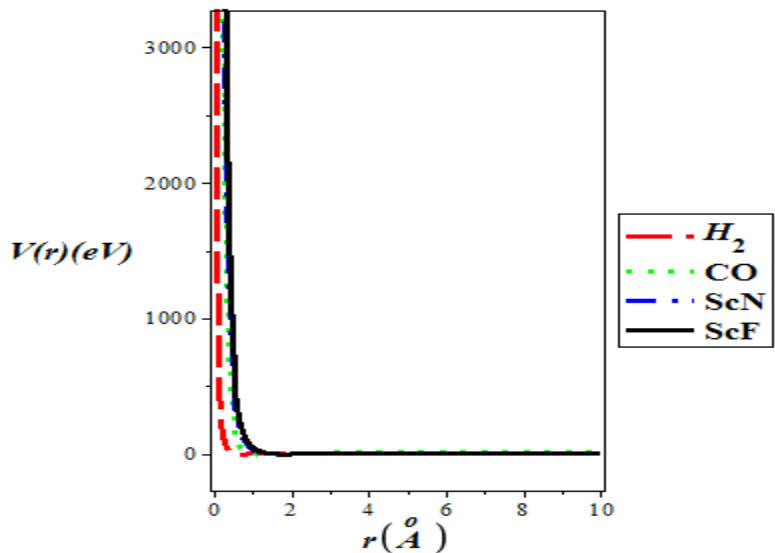


Figure 2: Shape of the Deng-Fan-Eckart diatomic molecular potential for different diatomic molecules.

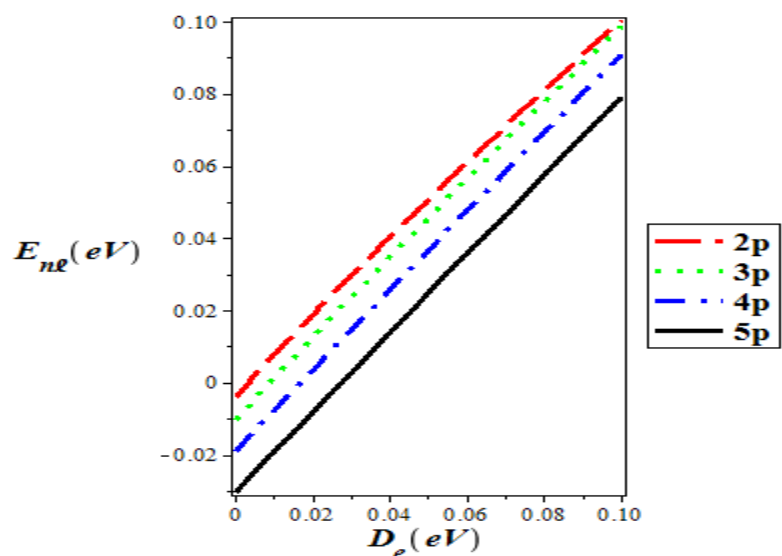


Figure 3: energy eigenvalues variation with dissociation energy for various quantum state

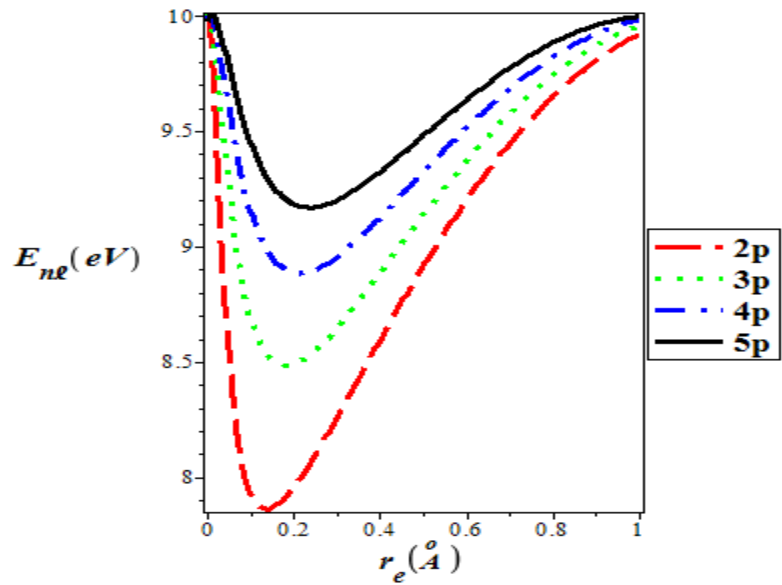


Figure 4: energy eigenvalues variation with equilibrium bond length for various quantum states

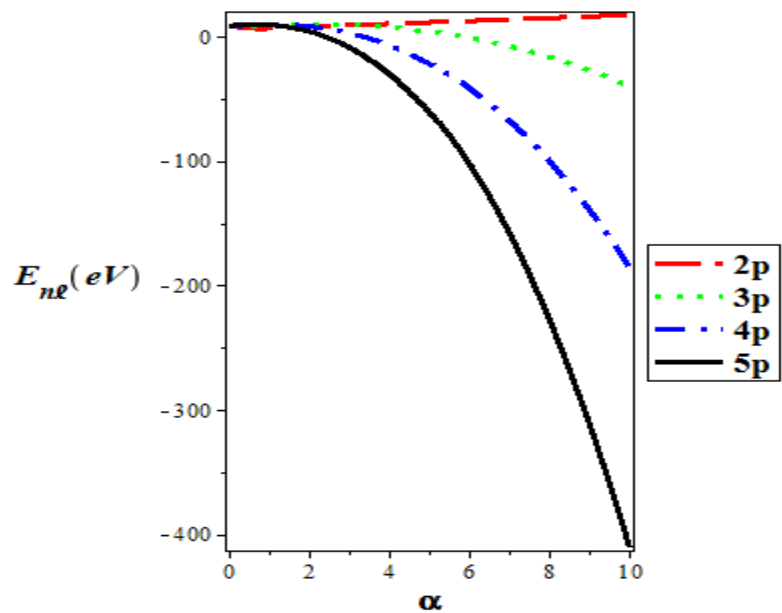


Figure 5: energy eigenvalues variation with screening parameter for various quantum states

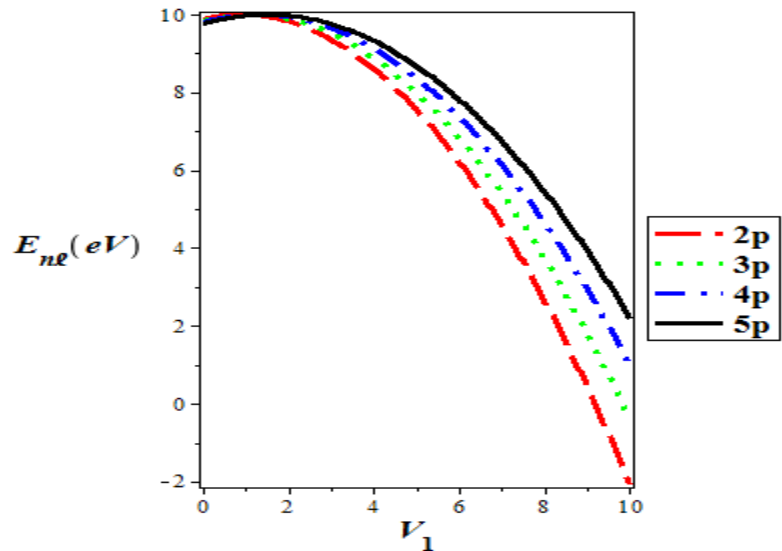


Figure 6: energy eigenvalues variation with parameter V_1 for various quantum states

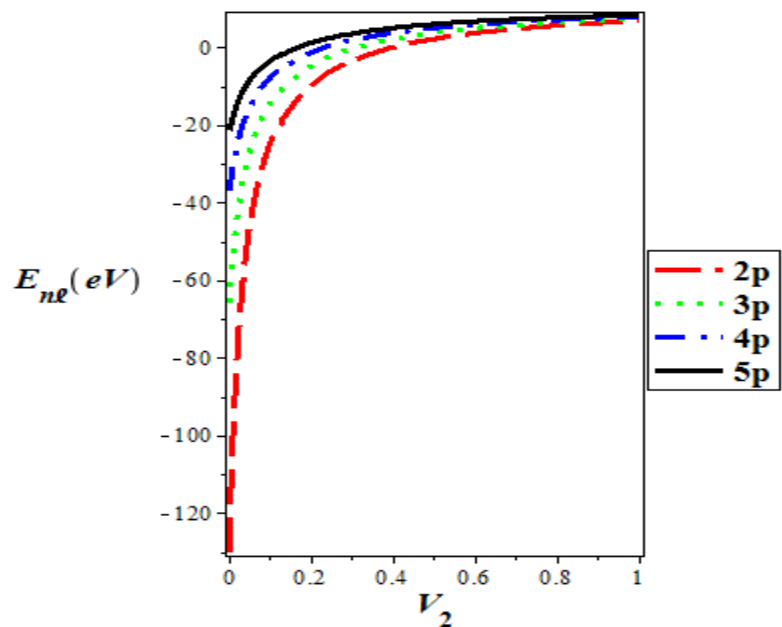


Figure 7:energy eigenvalues variation with parameter V_2 for various quantum states

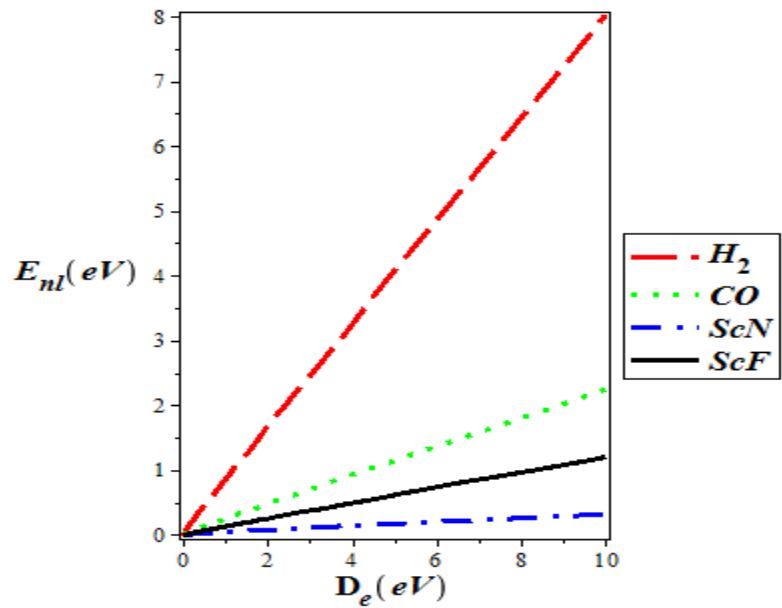


Figure 8: energy eigenvalues variation with dissociation energy for various diatomic molecules

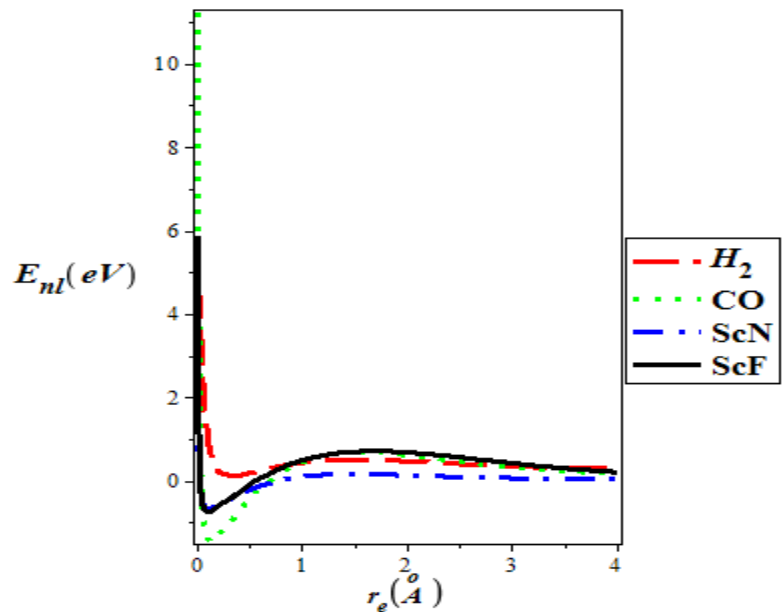


Figure 9: energy eigenvalues variation with equilibrium bond length for various diatomic molecules

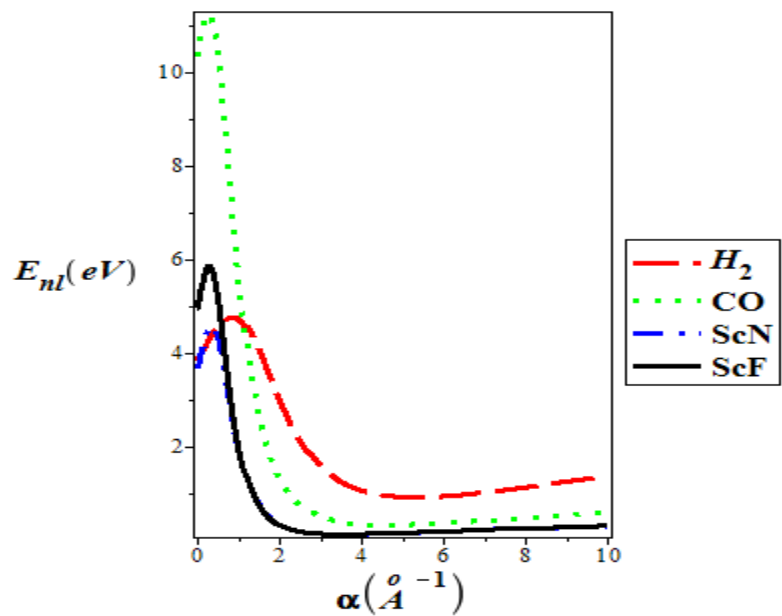


Figure 10: energy eigenvalues variation with screening parameter for various diatomic molecules

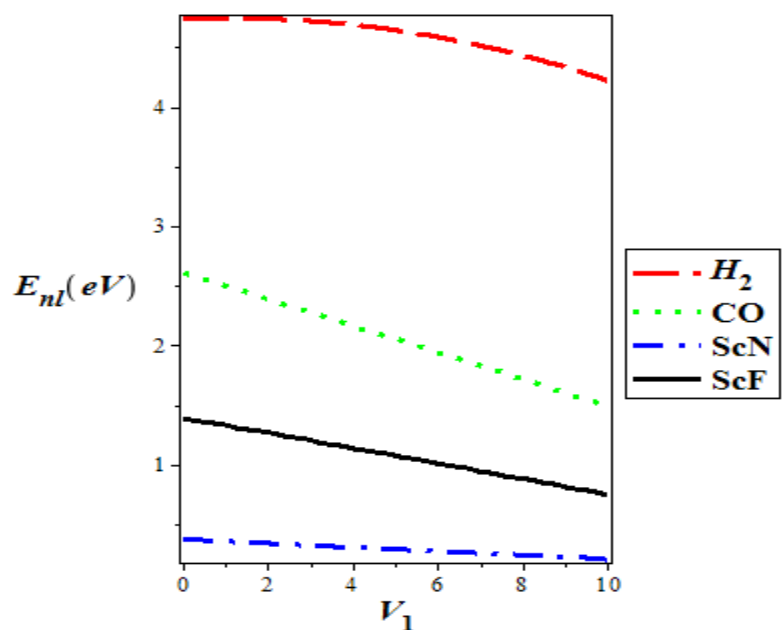


Figure 11: energy eigenvalues variation with the parameter V_1 for various diatomic molecules

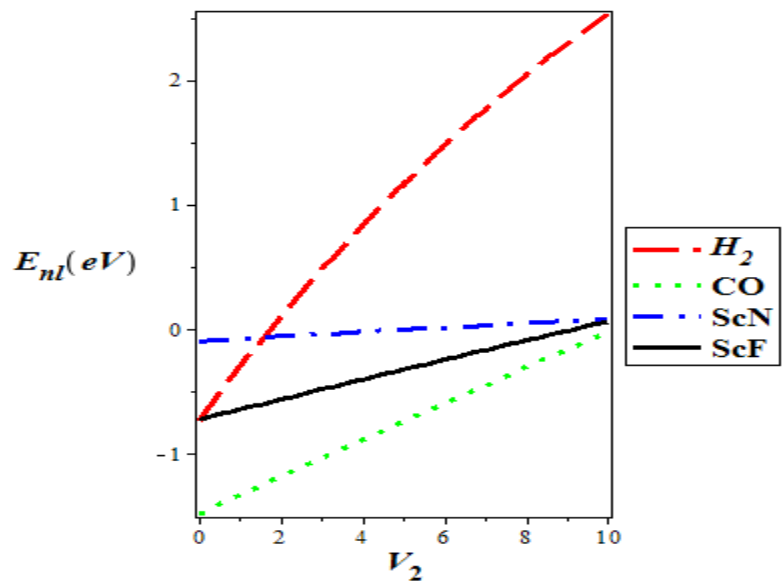


Figure 12: energy eigenvalues variation with the parameter V_2 for various diatomic molecules

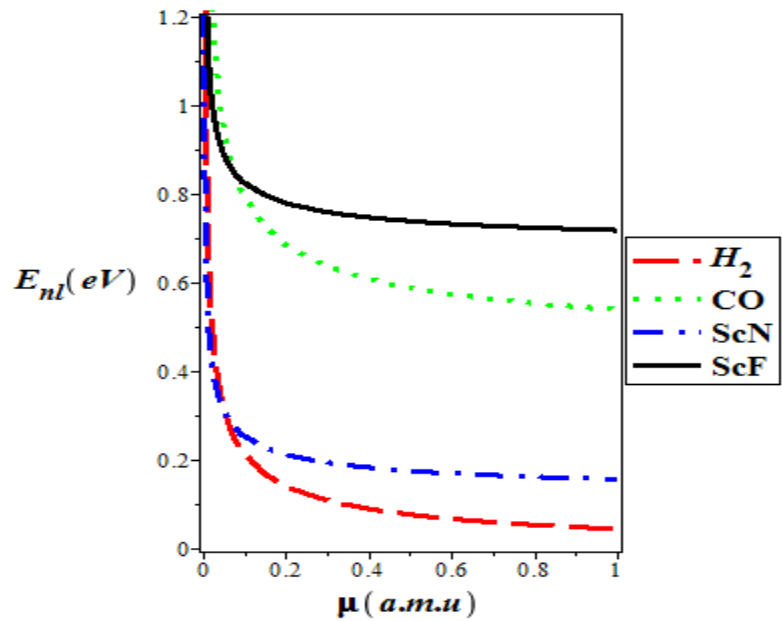


Figure 13: energy eigenvalues variation with the particle mass μ for various diatomic molecules

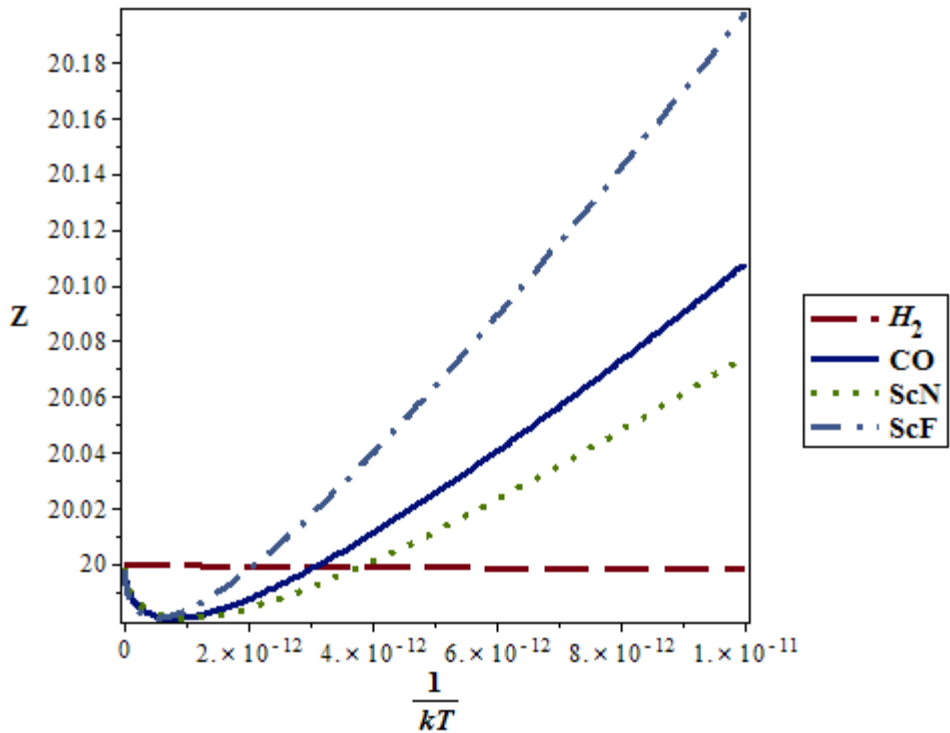


Figure 14: vibrational partition function variation with temperature for various diatomic molecules.

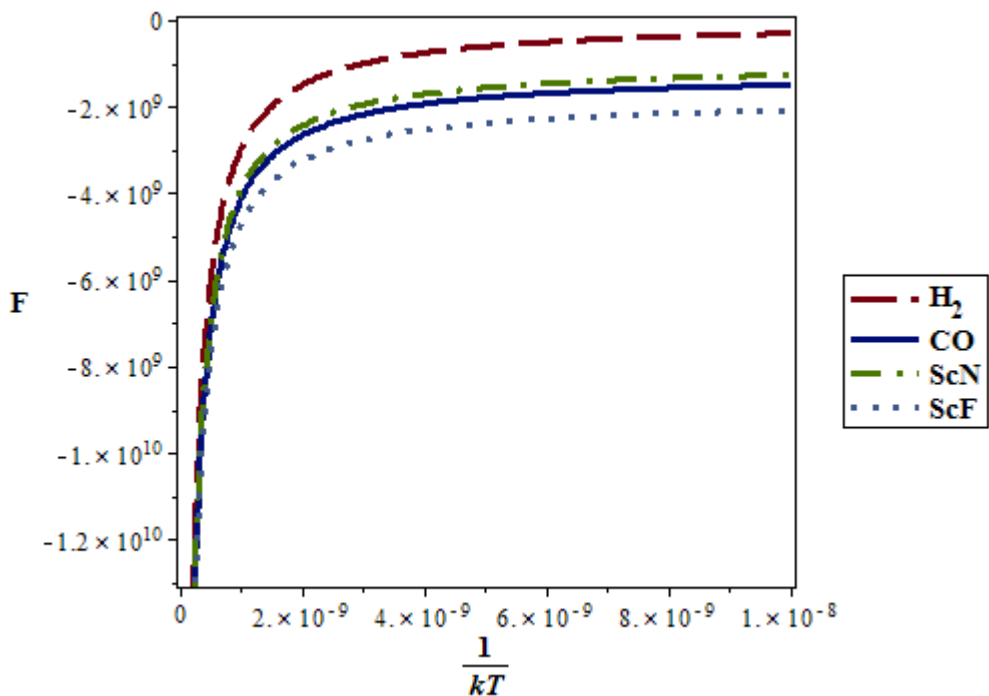


Figure 15: Vibrational free energy variation with temperature for various diatomic molecules.

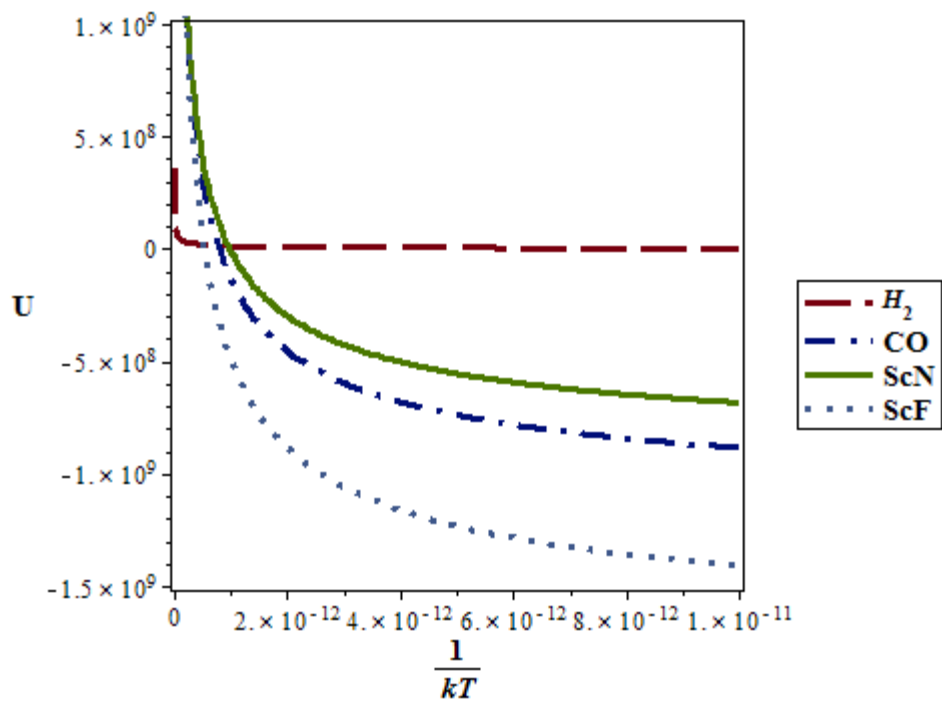


Figure 16: Vibrational mean energy variation with temperature for various diatomic molecules.

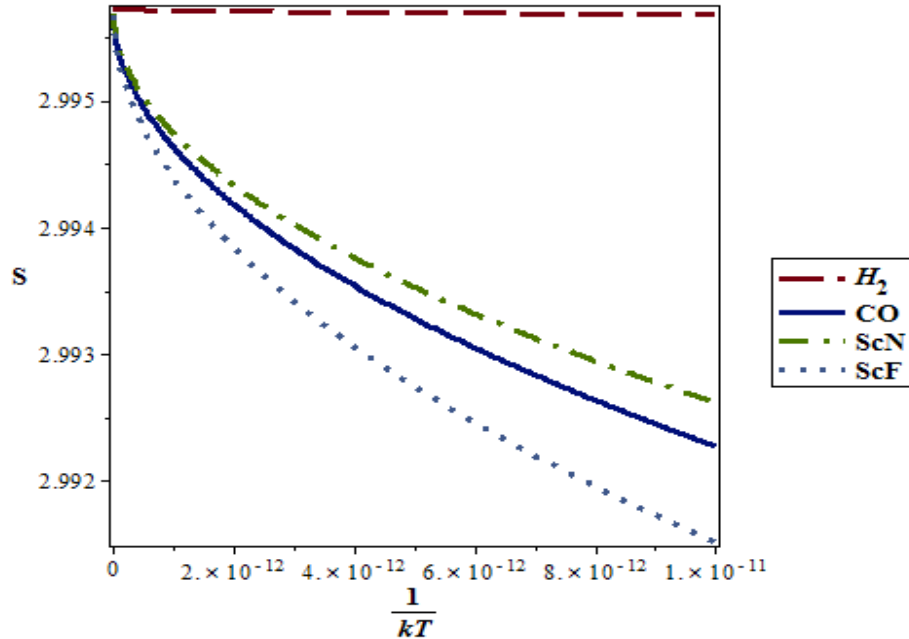


Figure 17: Vibrational entropy variation with temperature for various diatomic molecules.

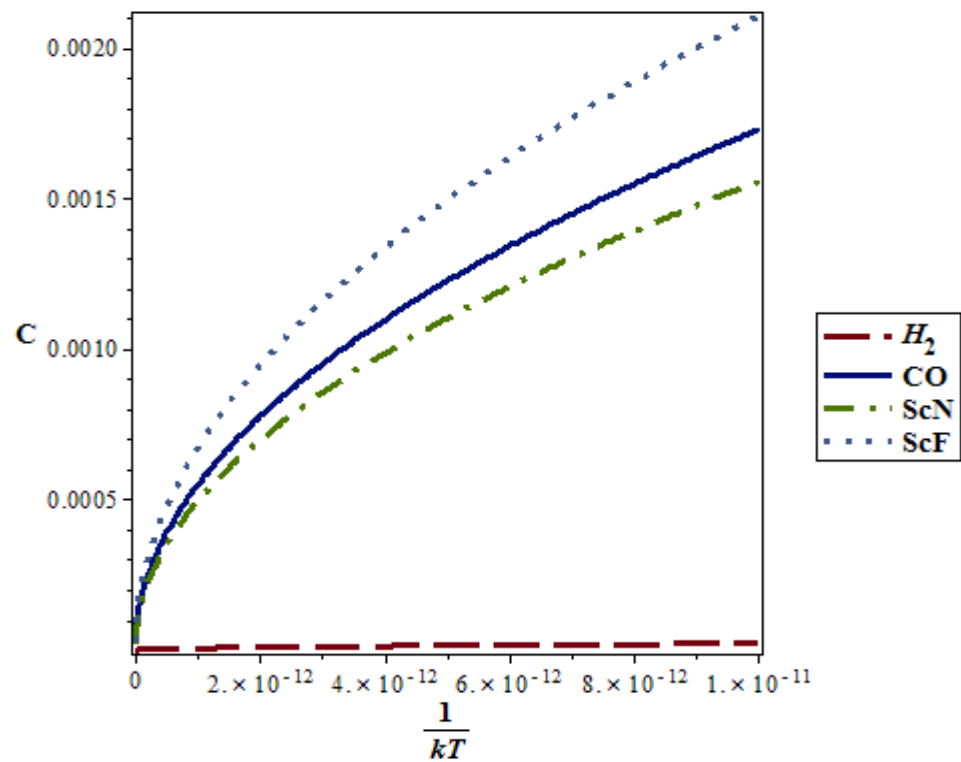


Figure 18: Vibrational specific heat capacity variation with temperature for various diatomic molecules.

Table 1; Spectroscopic parameters of the molecules used in this work

Parameters	H_2 [31]	CO [30]	ScN [31]	ScF [31]
$D_e (cm^{-1})$	38266	90540	36778.88	47183.43
$r_e (\text{\AA})$	0.7416	1.1283	1.768	1.794
$\alpha (\text{\AA}^{-1})$	1.9426	2.294	1.5068	1.46102
$\mu (a.m.u)$	0.50391	6.860672	10.68277	13.35894

Table 2. Comparison of energy eigenvalues (in eV) obtained by using Factorization Method with other methods for $2p$, $3p$, $3d$, $4d$, $4f$, $5p$, $5d$, $5f$, $5g$, $6p$, $6d$, $6f$ and $6g$ states in atomic units
 $\hbar = \mu = 1$ for $r_e = 0.4$ and $D_e = 15$.

states	α	Present	NU[31]	AIM[66]	EXACT[60]	FAA[60]	LXC[67]
2p	0.05	7.860804501	7.860804493	7.860804467	7.862800	7.86060	7.86080
	0.10	7.95330448	7.953304454	7.953304350	7.955370	7.95247	7.95330
	0.15	8.045099826	8.04509987	8.045099635	8.047240	8.04322	8.04510
	0.20	8.136203742	8.136203772	8.136203356	8.138420	8.13287	8.13620
	0.25	8.226629166	8.226629167	8.226628516	8.228920	8.22142	8.22660
	0.30	8.316389012	8.31638903	8.316388092	8.318740	8.30889	8.31639
3p	0.05	10.99776305	10.99776305	10.99776302	10.999800	10.99760	10.99780
	0.10	11.16256048	11.16256046	11.16256036	11.164700	11.16170	11.16260
	0.15	11.32424869	11.32424872	11.32424848	11.326470	11.32240	11.32420
	0.20	11.4828376	11.48283762	11.48283721	11.485130	11.47950	11.48280
	0.25	11.63833667	11.63833667	11.63833602	11.640680	11.63310	11.63830
	0.30	11.790755	11.79075502	11.79075408	11.675650	11.78330	11.79080
3d	0.05	10.21598027	10.21598027	10.21598019	10.216510	10.21540	10.21598
	0.10	10.3535395	10.35353947	10.35353916	10.354090	10.35100	10.35353
	0.15	10.48935435	10.48935439	10.48935369	10.489920	10.48370	10.48935
	0.20	10.62346372	10.62346374	10.62346249	10.624030	10.61350	10.62346
	0.25	10.75590641	10.75590641	10.75590446	10.756450	10.74030	10.75591
	0.30	10.88672148	10.88672151	10.88671869	10.887190	10.86420	10.88672
4p	0.05	12.49760242	12.49760242	12.4976024	12.499200	12.49740	12.49760
	0.10	12.69679606	12.69679604	12.69679594	12.698510	12.69600	12.69680
	0.15	12.88834811	12.88834813	12.8883479	12.890100	12.88650	12.88835
	0.20	13.07224461	13.07224462	13.0722442	13.074000	13.06890	13.07224
	0.25	13.24847044	13.24847044	13.24846979	13.250100	13.24330	13.24847
4d	0.05	12.09829027	12.09829027	12.09829019	12.098900	12.09770	12.09829
	0.10	12.28500944	12.28500942	12.2850091	12.285700	12.28250	12.28501
	0.15	12.46641934	12.46641937	12.46641867	12.467150	12.46080	12.46642
	0.20	12.64256754	12.64256756	12.64256631	12.643240	12.63260	12.64257
4f	0.05	11.82078624	11.82078623	11.82078608	11.820900	11.81950	11.82079
	0.10	11.99796123	11.99796121	11.99796058	11.998100	11.99300	11.99796
	0.15	12.17169657	12.17169661	12.1716952	12.171800	12.16040	12.17170
	0.20	12.34207215	12.34207217	12.34206967	12.342100	12.32210	12.34207
5p	0.10	13.54214251	13.5421425	13.5421424	13.543400	13.54130	13.54214
	0.20	13.92898632	13.92898633	13.92898591	13.930100	13.92570	13.92999
5d	0.10	13.30679692	13.3067969	13.30679659	13.307500	13.30430	13.30680
	0.20	13.69266394	13.69266395	13.6926627	13.693100	13.68270	13.69266
5f	0.10	13.14759773	13.14759771	13.14759709	13.147800	13.14260	13.14760
	0.20	13.53344224	13.53344225	13.53343975	13.533300	13.51340	13.53344

5g	0.10	13.03797622	13.03797622	13.03797516	13.037900	13.02960	13.03798
	0.20	13.42711264	13.42711266	13.4271085	13.426670	13.39380	13.42711
6p	0.10	14.05208861	14.05208861	14.0520885	14.053000	14.05130	14.05209
6d	0.10	13.90704847	13.90704846	13.90704815	13.907500	13.90450	13.90705
6f	0.10	13.81118996	13.81118995	13.81118932	13.811300	13.80620	13.81119
6g	0.10	13.74661284	13.74661283	13.74661179	13.746600	13.73830	13.74361

Table 3. Comparison of energy eigenvalues (in eV) obtained by using Factorization Method with other methods for $2p$, $3p$, $3d$, $4d$, $4f$, $5p$, $5d$, $5f$, $5g$, $6p$, $6d$, $6f$ and $6g$ states in atomic units
 $\hbar = \mu = 1$ for $r_e = 0.8$ and $D_e = 15$.

States	α	Present	NU[31]	AIM[66]	EXACT[60]	APPROXIMATE[60]	LXC[67]
2p	0.05	4.140887280	4.140887263	4.140887237	4.14208	4.14068	4.140887
	0.10	4.219180100	4.219180128	4.219180023	4.22040	4.21835	4.219180
	0.15	4.297393180	4.297393199	4.297392964	4.29870	4.29552	4.297393
	0.20	4.375546500	4.375546508	4.375546092	4.37690	4.37221	4.375547
	0.25	4.453659650	4.453659654	4.453659003	4.45510	4.44845	4.653660
	0.30	4.531751800	4.531751791	4.531750853	4.53320	4.52425	4.531752
3p	0.05	7.532791581	7.532791561	7.532791535	7.53500	7.53258	7.532792
	0.10	7.724764250	7.724764274	7.724764169	7.72710	7.72393	7.724764
	0.15	7.915178638	7.915178655	7.915178421	7.91770	7.9133	7.915179
	0.20	8.104040620	8.104040627	8.104040211	8.10660	8.10071	8.104041
	0.25	8.291354170	8.291354169	8.291353518	8.29410	8.28615	8.291354
	0.30	8.477121312	8.477121312	8.477120373	8.47990	8.46962	8.477121
3d	0.05	5.739751255	5.739751228	5.73975115	5.74040	5.73913	5.739751
	0.10	5.845770258	5.845770281	5.845769968	5.84650	5.84327	5.845770
	0.15	5.950678118	5.950678133	5.95067743	5.95150	5.94505	5.950678
	0.20	6.054533595	6.054533598	6.054532348	6.05530	6.04453	6.054534
	0.25	6.157395320	6.157395321	6.157393368	6.15820	6.14177	6.157395
	0.30	6.259321760	6.259321745	6.259318933	6.26010	6.23682	6.259322
4p	0.05	9.613013105	9.613013087	9.613013061	9.61560	9.6128	9.613013
	0.10	9.883523678	9.883523698	9.883523594	9.88620	9.88269	9.983524
	0.15	10.148555700	10.14855572	10.14855549	10.15140	10.1467	10.148560
	0.20	10.408057740	10.40805775	10.40805734	10.41110	10.4047	10.408060
	0.25	10.661973880	10.66197388	10.66197323	10.66500	10.6568	10.661970
4d	0.05	8.493343511	8.493343486	8.493343408	8.49480	8.49272	8.493344
	0.10	8.707110961	8.707110984	8.707110672	8.70870	8.70461	8.707111
	0.15	8.917807581	8.917807599	8.917806896	8.91940	8.91218	8.917808
	0.20	9.125505091	9.125505093	9.125503844	9.12720	9.11551	9.125505
4f	0.05	7.434705841	7.434705812	7.434705654	7.43510	7.43346	7.434706
	0.10	7.586418776	7.586418806	7.586418181	7.58680	7.58142	7.586419
	0.15	7.735732245	7.735732273	7.735730867	7.73610	7.72448	7.735732
	0.20	7.882757509	7.882757512	7.882755012	7.88310	7.86276	7.882758
5p	0.10	11.302072420	11.30207244	11.30207233	11.30470	11.3012	11.302070
	0.20	11.913223740	11.91322375	11.91322333	11.91610	11.9099	11.913220
5d	0.10	10.520086060	10.52008608	10.52008576	10.52190	10.5176	10.520090
	0.20	11.069371600	11.06937161	11.06937036	11.07130	11.0594	11.069370
5f	0.10	9.796658009	9.796658033	9.796657408	9.79750	9.79166	9.796658
	0.20	10.273037060	10.27303707	10.27303457	10.27380	10.253	10.273040

5g	0.10	9.152223325	9.152223355	9.15222313	9.15240	9.14389	9.522230
	0.20	9.552869470	9.552869479	9.552865312	9.55280	9.51954	9.552869
6p	0.10	12.279799200	12.27979921	12.27979911	12.28220	12.279	12.279800
6d	0.10	11.736438620	11.73643864	11.73643833	11.73830	11.7339	11.736440
6f	0.10	11.244814900	11.24481492	11.2448143	11.24590	11.2398	11.244810
6g	0.10	10.815332260	10.81533228	10.81533124	10.81580	10.807	10.815330

Table 4: The bound state energies E_{nl} (eV) for H_2 , CO , ScN and ScF molecules for different values of the vibrational n and rotational ℓ quantum numbers of the Deng–Fan–Eckart potential

n	ℓ	H_2	CO	ScN	ScF
0	0	0.3161089	0.3653484	0.5678234	0.7807499
0	1	0.3304972	0.3658917	0.5679634	0.7808573
1	0	0.9626475	0.6487759	0.6573524	0.8685782
1	1	0.9759181	0.6493153	0.6574917	0.8686851
2	0	1.5466492	0.9281700	0.7457977	0.9555848
2	1	1.5588663	0.9287056	0.7459361	0.9556913
2	2	1.5832386	0.9297766	0.7462130	0.9559042
3	0	2.0716668	1.2035434	0.8331616	1.0417712
3	1	2.0828895	1.2040751	0.8332993	1.0418772
3	2	2.1052768	1.2051383	0.8335745	1.0420891
3	3	2.1387131	1.2067333	0.8339876	1.0424072
4	0	2.5409692	1.4749081	0.9194467	1.1271390
4	1	2.5512519	1.4754360	0.9195836	1.1272445
4	2	2.5717628	1.4764914	0.9198573	1.1274555
4	3	2.6023934	1.4780750	0.9202679	1.1277721
4	4	2.6429822	1.4801861	0.9208153	1.1281941
5	0	2.9575685	1.7422767	1.0046555	1.2116896
5	1	2.9669614	1.7428007	1.0047916	1.2117947
5	2	2.9856959	1.7438485	1.0050637	1.2120047
5	3	3.0136703	1.7454204	1.0054720	1.2123199
5	4	3.0507328	1.7475162	1.0060162	1.2127400
5	5	3.0966829	1.7501360	1.0066966	1.2132652